ESTEEM Academic Journal
Vol. 17, August 2021, 23-31

Amorphous Phase of SnO_2 doped Al_2O_3 thin film: Optical and Structural Properties

Puteri Sarah Mohamad Saad[1], Muhammad Nizar Aiman Mohd Zani[2], Anees Aziz[3] and Hashimah Hashim[4]
[1,2,3]NANO-ElecTronic Centre, School of Electrical Engineering, College of Engineering, Universiti Teknologi MARA, 40450 Shah Alam, Selangor, Malaysia
[4]School of Electrical Engineering, College of Engineering, Universiti Teknologi MARA, 40450 Shah Alam, Selangor, Malaysia
**corresponding author: [1]puterisarah@uitm.edu.my*

ARTICLE HISTORY

Received
24 May 2021

Accepted
27 June 2021

Available online
4 August 2021

ABSTRACT

Tin Oxide (SnO_2) is an n-type semiconductor with a direct bandgap of 3.6eV. It is highly conductive, transparent, and gas sensitive. The SnO_2 can be unstable depending on certain parameters and methods to prepare it. In this work, the thin film of SnO_2 doped with Al_2O_3 was deposited by electrospinning on glass substrates. The thin films were then annealed at 100°C, 200°C, 300°C, 400°C, 500°C, and then the optical and physical films were examined. Measurements of X-Ray Diffraction (XRD) and Microscope were performed for structural and morphological analysis. The optical characteristics were analyzed using the UV-Vis spectrophotometer. As the annealing temperature increases, the optical transmittance also increases due to the increase in film homogeneity and the degree of crystallinity of the film. The rise in temperature leads to a decrease in absorption values.

Keywords: *SnO_2, Al_2O_3, Amorphous, Annealing temperature, Electrospinning.*

1. INTRODUCTION

Semiconductors are one of the most interesting and useful solids. They have been investigated many times for their flexibility, electrical characteristics, and optical characteristics. SnO_2 is included in the semiconductor group and has a large bandgap (3.6 – 4.0eV) [1-3]. SnO_2 can be used in many applications, such as solar cells and gas sensors [4-7], due to the large bandgap. In addition to its electronic properties, SnO_2 also has unique optical properties [8, 9]. Among other n-type oxide materials, SnO_2 is most used in gas sensors to detect gas concentrations [10]. The practical performance of SnO_2 is dependent on its morphology, crystal defects, surface properties, and crystal size. It is therefore necessary to control the morphology and size during preparation in order to obtain the required chemical and physical properties [11-13].

There are many ways to prepare a thin SnO_2 film. Several synthesis techniques have been used, such as solvothermal [14], co-precipitation [15, 16], sol-gel [17, 18] hydrothermal [19, 20], solid-state reaction technique [21] and, microwave-assisted nanostructure preparation [22]. Sol-gel-dip coatings, spray pyrolysis, pulsed deposition, and sputtering [23] are among the sol-gel method. In addition, electrospinning can also be used to produce a thin SnO_2 film. Among these, we employed the electrospinning method to synthesize SnO_2 nanostructures as it has several advantages such as that it has been reported to have successfully produced SnO_2 in the form of nanofibers [24], a simple and versatile method to produce nanofiber from a wide range of materials, including polymers, composites, and ceramics [25]. Apart from producing homogeneous particles, this method is cheap and does not require any complicated tools.

p-ISSN 1675-7939; e-ISSN 2289-4934

Electrospinning is a manufacturing technique involving an electrostatic driven process used to produce electrospun fibers. It is a very simple technique to produce fibers ranging from submicron to nanometre [26, 27]. In electrospinning, solid fiber is produced by continuous stretching of the electrified jet due to electrostatic repulsions between surface loads and solvent evaporation [25]. The solution formed at the end of the metal tip is highly electrified by a strong electrical field. This technique required high voltage to induce the formation of a liquid jet.

However, SnO_2 is not stable due to its wide bandgap, and to make the nanomaterial more stable, it must undergo doping and an annealing process [28-31]. Previous work has been reported on how annealing temperature can change the properties of SnO_2 [32, 33]. Among the studies that have been conducted, it has been shown how annealing temperature can reduce the intrinsic stress, improve the uneven distribution between the lattices and create a longer mean path for free electrons to improve electrical conductivity [34] due to the improved mobility of the carriers. High annealing temperature effects [35] should be considered to improve nanocrystalline films and increase the particle size. Moreover, the high annealing temperatures may increase the diffraction peak intensity to become sharper and stronger. This may be due to a decrease in film homogeneity and the degree of crystallinity of the film [36]. The results show that a higher annealing temperature results in a lower surface roughness and larger crystal size [7].

Amorphous SnO_2 is usually produced at low temperatures. It is defined as a formless or undefined material where it is not easy to determine the characteristics or properties of the material. Therefore, it is not preferable to use material with this form in some electronic devices. The conductivity of this type of material is also low and it will not exhibit good electrical properties. SnO_2, which has been deposited at such high temperatures, exhibits good electronic and optical properties, however, such high temperatures cannot be used for all applications. For example, for a film on temperature-sensitive substrates (plastic) or the deposition of SnO_2 films on active devices, such as thin film solar cells or photoelectrodes. In such cases, low-temperature deposition processes, such as the reactive magnetron sputtering, are required [37, 38].

In the work presented, the effect of SnO_2 doped Al_2O_3 thin film deposited by electrospinning at different annealing temperatures (100°C, 200°C, 300°C, 400°C, 500°C) is investigated. It focused mainly on physical and optical properties.

2. METHODOLOGY

This section describes the preparation of thin film samples of SnO_2 doped Al_2O_3 from start to finish. The preparation process begins with the preparation of SnO_2 doped Al_2O_3 solution. The next step is to prepare a SnO_2 doped Al_2O_3 thin film using the electrospinning method until it underwent the annealing process. Finally, the characterization process for these SnO_2 doped Al_2O_3 thin films is described.

2.1 *Preparation of SnO_2 doped 10 wt% Al_2O_3 solution*

To begin with, two solutions X and Y were prepared. A digital scale was used to weigh the tin (II) chloride ($SnCl_2H_2O$) and the Aluminum (III) Oxide powder.

Solution X was prepared by dissolving 1.5 g of $SnCl_2H_2O$ and 0.08066 g (10 *wt%*) of Al_2O_3 in 7.91 ml of 1.0M Ethyl Alcohol. It was stirred with a magnetic stirrer, set to 300 rpm, and placed

p-ISSN 1675-7939; e-ISSN 2289-4934

on a hot plate at 80 ^{o}C for two (2) hours. Furthermore, it was aged at room temperature for two (2) hours.

For solution Y, 1.5 g of polyvinylpyrrolidone (PVP) was dissolved in 7.5 ml ethanol and 7.5 ml Dimethylformamide (CH3)2NC(O)H. The solution was stirred with a magnetic stirrer at 300 rpm. In addition, it was placed on a digital hot plate stirrer for two (2) hours at 80 ^{o}C. Next, it was aged at room temperature for two (2) hours.

Finally, both solutions were mixed and stirred at 300 rpm for 24 hours at room temperature on a digital hot plate stirrer.

2.2 Preparation of SnO_2 doped 10 wt% Al_2O_3 thin film

The solution of SnO_2 doped 10 *wt%* Al_2O_3 was deposited on 2.5 cm x 2.5 cm glass substrates via the electrospinning method. The experimental setup for the electrospinning to prepare the SnO_2 doped 10 *wt%* Al_2O_3 thin film is shown in Figure 1. In this work, the Al_2O_3 was set to 10 *wt%* as discussed in Section 2.1. The solution was first filled in a syringe (10 cc/ml) with a 16G tip of a stainless needle.

Second, the syringe was placed on the syringe pump and a high voltage of 18 kV was applied to the 16G needle. The syringe pump and target rate were then set at 0.250 ml/h and 0.5 ml/h respectively. While the rotary drum machine was set to rotate the glass substrates at 250 rpm, the distance between the needle tip and the glass substrates was measured at 10 cm. When the voltage was applied to the tip and the collective target plate, the fluid jet was ejected from the tip of the needle.

The SnO_2 doped 10 wt% Al_2O_3 thin film deposition process took 1 hour to complete. Finally, all samples were annealed in a vertical furnace at 100°C, 200°C, 300°C, 400°C, 500°C for one (1) hour.

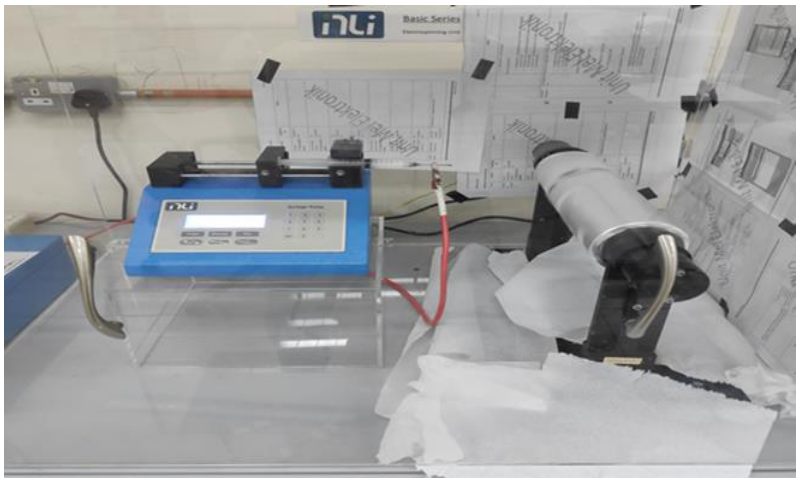

Figure 1: Electrospinning set up to prepare the SnO_2 doped Al_2O_3 thin film

p-ISSN 1675-7939; e-ISSN 2289-4934

2.3 Thin-film Characterizations

Descriptions of characterizations of the thin films are discussed in this section. The characterizations that were carried out were physical and optical properties. The optical properties of the thin films were analyzed using Ultraviolet-Visible Spectroscopy (UV-Vis) for all samples in the 300-800 nm range. Whereas the crystallinity characteristics were examined by X-ray diffraction (XRD) and the surface morphology was observed by a microscope.

3. RESULT AND DISCUSSION

3.1 Microscope measurement

Figure 2 depicts microscope images featuring SnO_2 doped Al_2O_3 thin film surface morphology at different annealing temperatures. A nanofiber-like structure for each sample was observed in the microscope images. The average diameter obtained from microscope images below 50 x magnification is shown to be 580, 493, 693, 650, 383 and 360 nm at 25°C, 100°C, 200°C, 300°C, 400°C, 500°C, respectively. The value of the diameter is shown in Table 1. As illustrated in Table 1, the diameter size showed a decrease in value as the annealing temperature increased from 25°C to 500°C. The reduction in grain size can be attributed to the improved crystal quality as the annealing temperature increased [39].

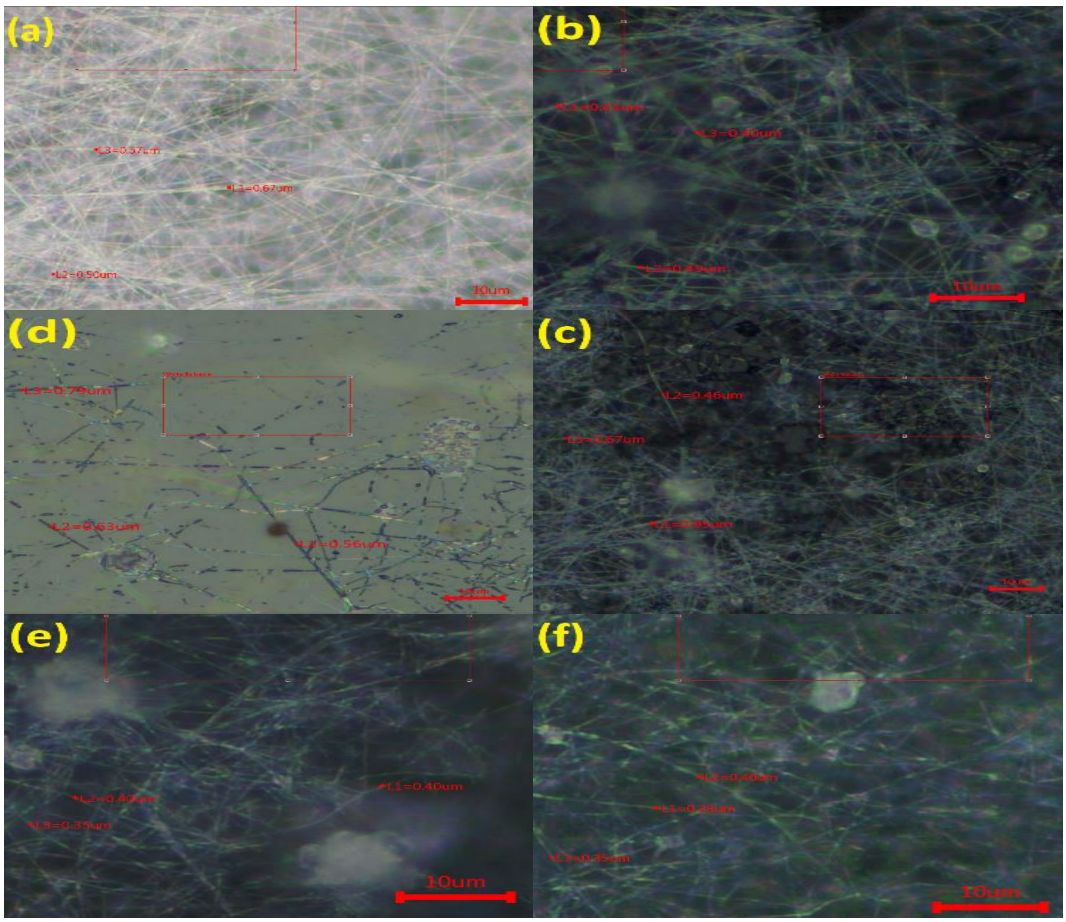

Figure 2: Microscope images of SnO_2 doped 10% Al_2O_3 under 50x magnification at different annealing temperatures (a) 25°C, (b) 100°C, (c) 200°C, (d) 300°C, (e) 400°C, and (f) 500°C

p-ISSN 1675-7939; e-ISSN 2289-4934

Table 1: The average diameter size for different annealing temperature

Temperature (°C)	Average diameter size (nm)
25	580
100	493
200	693
300	650
400	383
500	360

3.2 XRD Analysis

Figure 3 shows the XRD pattern for all samples at which revealed the amorphous or non-crystalline solid concerning the increased annealing temperature. Furthermore, all samples showed broad humps at $2\theta = 28^{o}$. The width of the humps is similar for all samples as the annealing temperature increased. Two possible explanations are that the annealing temperature is low and that the average crystalline size decreases as the molar concentration increases [40]. According to [36], the best temperature for SnO_2 preparation is above 500 ^{o}C. It has also been reported that as annealing temperature increases, the intensity of diffraction peaks increases and becomes sharper and stronger [37]. We conclude that the low annealing temperature is closer to the amorphous phase transformation than to the crystalline phase.

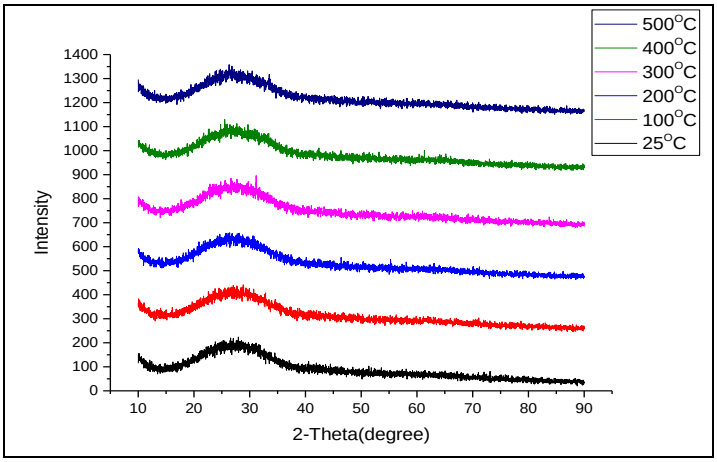

Figure 3: XRD pattern of SnO_2 doped wt% Al_2O_3 at different annealing temperatures 25°C, 100°C, 200°C, 300°C, 400°C, 500°

3.3 Optical Properties

Figure 4 shows the optical transmittance spectra of SnO_2 doped 10 *wt%* Al_2O_3 thin film deposited with various annealing temperatures. The transmission of all samples was between 14 T% and 62 T% at 350 nm wavelength. The optical transmittance has not increased or decreased as the annealing temperature increased. The highest transmittance was found at 350°C, with 62 T%, and the lowest transmittance was found at 100 ^{o}C, with 14 T%. This is due to the amorphous phase of SnO_2 doped Al_2O_3 obtained in this work. As reported elsewhere, when annealing temperature increases, the transmittance increases due to the increment in film

p-ISSN 1675-7939; e-ISSN 2289-4934

homogeneity and the degree of crystallinity of the film. From Fig. 3, with 500°C annealing temperature, it can be observed that there is a peak shift to a shorter wavelength (blue shift) [38]. These results are in agreement with the previous research [41, 42].

Figure 5 shows the absorbance spectra for all samples of SnO_2 doped 10 *wt%* Al_2O_3 thin film at different annealing temperatures. Showing clearly from this figure, the nanoparticles have a low absorbance value of 0.24 for 300 ℃ annealing temperature and a maximum absorbance value of 1.0 for 100 ℃ annealing temperature at 350 nm wavelength. All measurements were made within the visible range (300 – 800 nm). The absorbance edge (peak) shifted to a shorter wavelength when a high annealing temperature was applied to the sample. Figure 5 does not show an increase in the annealing temperature leading to a decrease in absorption values as the samples are in an amorphous phase. Both Figure 4 and Figure 5 show a significant increase at 200 – 300 ^oC, which could be attributed to the sample's treatment process at 200 ^oC, whereas at 300 ^oC onwards, it begins the annealing process, which modifies a material's microstructure to change its mechanical or electrical properties.

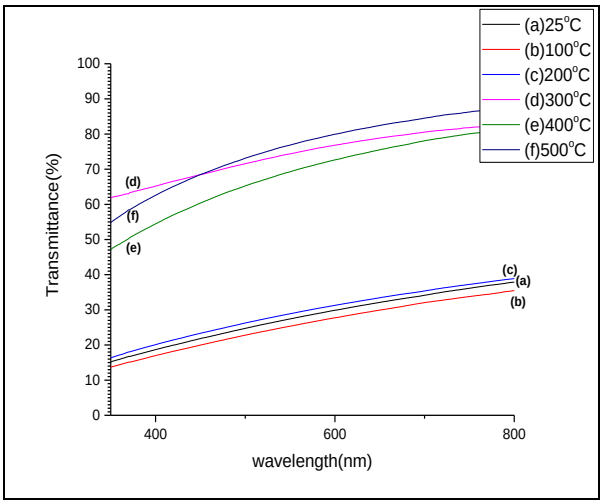

Figure 4: Transmittance spectra of SnO_2 doped *wt%* Al_2O_3 at different annealing temperatures 25°C, 100°C, 200°C, 300°C, 400°C, 500°.

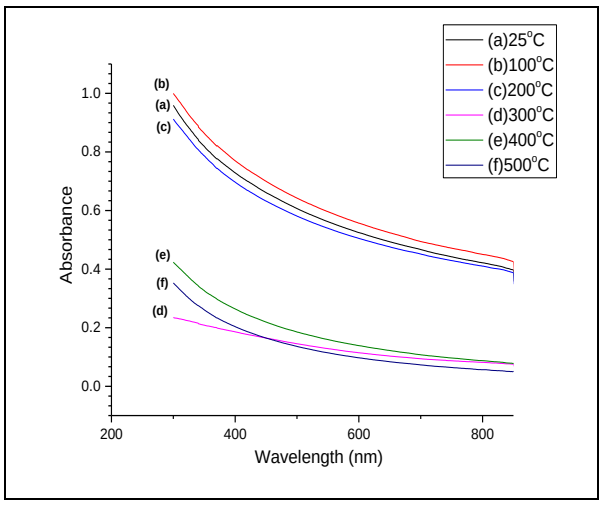

Figure 5: Absorbance spectra of SnO_2 doped *wt%* Al_2O_3 at different annealing temperatures 25°C, 100°C, 200°C, 300°C, 400°C, 500°C

p-ISSN 1675-7939; e-ISSN 2289-4934

4. CONCLUSION

SnO_2 doped Al_2O_3 was successfully deposited on glass substrates using the electrospinning method with different annealing temperatures. The fiber – look structure showed a reduced diameter and the XRD pattern showed an amorphous peak as the annealing temperature increased. While the optical properties are concluded, there is a peak shift to a shorter wavelength at an annealing temperature of 500 ℃.

ACKNOWLEDGEMENT

The authors would like to express their deepest appreciation to all the staff of the NANO-ElecTronic Center (NET) and the NANO-SciTech Center (NST) for their assistance in completing this work. Also, thanks to the FRGS financial support grant (FRGS/1/2019/TK04/UITM/02/44).

REFERENCES

[1] L. Nehru, V. Swaminathan, and C. Sanjeeviraja, "Photoluminescence studies on nanocrystalline tin oxide powder for optoelectronic devices," *American Journal of Materials Science*, vol. 2, no. 2, pp. 6-10, 2012.

[2] T. Krishnakumar, R. Jayaprakash, V. Singh, B. Mehta, and A. Phani, "Synthesis and characterization of tin oxide nanoparticle for humidity sensor applications," in *Journal of Nano Research*, vol. 4: Trans Tech Publ, pp. 91-101, 2008.

[3] A. F. Khan, M. Mehmood, M. Aslam, and M. Ashraf, "Characteristics of electron beam evaporated nanocrystalline SnO2 thin films annealed in air," *Applied Surface Science*, vol. 256, no. 7, pp. 2252-2258, 2010.

[4] A. Cirera, A. Vila, A. Dieguez, A. Cabot, A. Cornet, and J. Morante, "Microwave processing for the low cost, mass production of undoped and in situ catalytic doped nanosized SnO_2 gas sensor powders," *Sensors and Actuators B: Chemical*, vol. 64, no. 1-3, pp. 65-69, 2000.

[5] N. K. Huu, D.-Y. Son, I.-H. Jang, C.-R. Lee, and N.-G. Park, "Hierarchical SnO_2 nanoparticle-ZnO nanorod photoanode for improving transport and life time of photoinjected electrons in dye-sensitized solar cell," *ACS applied materials & interfaces*, vol. 5, no. 3, pp. 1038-1043, 2013.

[6] Y. Liu, Y. Jiao, Z. Zhang, F. Qu, A. Umar, and X. Wu, "Hierarchical SnO_2 nanostructures made of intermingled ultrathin nanosheets for environmental remediation, smart gas sensor, and supercapacitor applications," *ACS applied materials & interfaces*, vol. 6, no. 3, pp. 2174-2184, 2014.

[7] C.-F. Liu, C.-H. Kuo, T.-H. Chen, and Y.-S. Huang, "Optoelectronic Properties of Ti-doped SnO_2 Thin Films Processed under Different Annealing Temperatures," *Coatings*, vol. 10, no. 4, p. 394, 2020. [Online]. Available: https://www.mdpi.com/2079-6412/10/4/394.

[8] H. Pang, H. Yang, C. X. Guo, and C. M. Li, "Functionalization of SnO2 photoanode through Mg-doping and TiO2-coating to synergically boost dye-sensitized solar cell performance," *ACS applied materials & interfaces*, vol. 4, no. 11, pp. 6261-6265, 2012.

[9] K. Suematsu *et al.*, "Nanoparticle cluster gas sensor: controlled clustering of SnO2 nanoparticles for highly sensitive toluene detection," *ACS applied materials & interfaces*, vol. 6, no. 7, pp. 5319-5326, 2014.

[10] N. Yamazoe, "Toward innovations of gas sensor technology," *Sensors and Actuators B: Chemical*, vol. 108, no. 1-2, pp. 2-14, 2005.

p-ISSN 1675-7939; e-ISSN 2289-4934

[11] H. Kaur, H. Bhatti, and K. Singh, "Effect of organic solvents on photocatalytic activity of PEG-capped SnO 2 nanoparticles," *Journal of Materials Science: Materials in Electronics,* vol. 29, no. 3, pp. 2026-2034, 2018.
[12] V. Kumar *et al.*, "Effect of solvent on crystallographic, morphological and optical properties of SnO2 nanoparticles," *Materials Research Bulletin,* vol. 85, pp. 202-208, 2017.
[13] C. A. Ibarguen, A. Mosquera, R. Parra, M. Castro, and J. Rodríguez-Páez, "Synthesis of SnO2 nanoparticles through the controlled precipitation route," *Materials Chemistry and Physics,* vol. 101, no. 2-3, pp. 433-440, 2007.
[14] L. Xia *et al.*, "High-yield solvothermal synthesis of single-crystalline tin oxide tetragonal prism nanorods," *Materials Letters,* vol. 61, no. 4-5, pp. 1214-1217, 2007.
[15] G. Singh and R. C. Singh, "Synthesis and characterization of Gd-doped SnO2 nanostructures and their enhanced gas sensing properties," *Ceramics International,* vol. 43, no. 2, pp. 2350-2360, 2017.
[16] Y. Li, J. Wang, B. Feng, K. Duan, and J. Weng, "Synthesis and characterization of antimony-doped tin oxide (ATO) nanoparticles with high conductivity using a facile ammonia-diffusion co-precipitation method," *Journal of Alloys and Compounds,* vol. 634, pp. 37-42, 2015.
[17] T. Duan, Q. Wen, Y. Chen, Y. Zhou, and Y. Duan, "Enhancing electrocatalytic performance of Sb-doped SnO2 electrode by compositing nitrogen-doped graphene nanosheets," *Journal of hazardous materials,* vol. 280, pp. 304-314, 2014.
[18] K. Sakthiraj and M. Hema, "Enhancement of room temperature ferromagnetism in tin oxide nanocrystal using organic solvents," *Applied Surface Science,* vol. 420, pp. 145-153, 2017.
[19] M. A. Akhir, K. Mohamed, H. Lee, and S. A. Rezan, "Synthesis of tin oxide nanostructures using hydrothermal method and optimization of its crystal size by using statistical design of experiment," *Procedia Chemistry,* vol. 19, pp. 993-998, 2016.
[20] R. Mishra *et al.*, "SnO 2 quantum dots decorated on RGO: A superior sensitive, selective and reproducible performance for a H 2 and LPG sensor," *Nanoscale,* vol. 7, no. 28, pp. 11971-11979, 2015.
[21] E. Tan, G. Ho, A. Wong, S. Kawi, and A. Wee, "Gas sensing properties of tin oxide nanostructures synthesized via a solid-state reaction method," *Nanotechnology,* vol. 19, no. 25, pp. 255706, 2008.
[22] M. Akram, A. T. Saleh, W. A. W. Ibrahim, A. S. Awan, and R. Hussain, "Continuous microwave flow synthesis (CMFS) of nano-sized tin oxide: Effect of precursor concentration," *Ceramics International,* vol. 42, no. 7, pp. 8613-8619, 2016.
[23] S. Baco, A. Chik, and F. M. Yassin, "Study on optical properties of tin oxide thin film at different annealing temperature," *Journal of Science and Technology,* vol. 4, no. 1, 2012.
[24] S.-W. Choi, J. Zhang, K. Akash, and S. S. Kim, "H2S sensing performance of electrospun CuO-loaded SnO2 nanofibers," *Sensors and Actuators B: Chemical,* vol. 169, pp. 54-60, 2012.
[25] D. Li and Y. Xia, "Electrospinning of nanofibers: reinventing the wheel?," *Advanced materials,* vol. 16, no. 14, pp. 1151-1170, 2004.
[26] J. M. Themlin, R. Sporken, J. Darville, R. Caudano, J. Gilles, and R. Johnson, "Resonant-photoemission study of SnO 2: cationic origin of the defect band-gap states," *Physical Review B,* vol. 42, no. 18, pp. 11914, 1990.
[27] J. Joseph, V. Mathew, J. Mathew, and K. Abraham, "Studies on Physical Properties and Carrier Conversion of SnO_2: Nd Thin Films," *Turkish Journal of Physics,* vol. 33, no. 1, pp. 37-47, 2009.
[28] A. Azam, A. S. Ahmed, S. S. Habib, and A. Naqvi, "Effect of Mn doping on the structural and optical properties of SnO2 nanoparticles," *Journal of Alloys and Compounds,* vol. 523, pp. 83-87, 2012.
[29] S. Kumar *et al.*, "Tailoring the structural, electronic structure and optical properties of Fe: SnO2 nanoparticles," *Journal of Electron Spectroscopy and Related Phenomena,* vol. 240, pp. 146934, 2020.

p-ISSN 1675-7939; e-ISSN 2289-4934

[30] A. G. Habte, F. G. Hone, and F. B. Dejene, "Influence of annealing temperature on the structural, morphological and optical properties of SnO2 nanoparticles," *Physica B: Condensed Matter*, vol. 580, pp. 411760, 2020.
[31] H. Mallick, Y. Zhang, J. Pradhan, M. Sahoo, and A. Pattanaik, "Influence of particle size and defects on the optical, magnetic and electronic properties of Al doped SnO2 nanoparticles," *Journal of Alloys and Compounds*, vol. 854, pp. 156067, 2021.
[32] S. Kaya, "Evolutions on surface chemistry, microstructure, morphology and electrical characteristics of SnO2/p-Si heterojuction under various annealing parameters," *Journal of Alloys and Compounds*, vol. 778, pp. 889-899, 2019.
[33] H. Kösea, A. Aydina, and H. Akbulutb, "The E ect of Temperature on Grain Size of SnO2 Nanoparticles Synthesized by Sol Gel Method," 2014.
[34] S. Mishra, C. Ghanshyam, N. Ram, S. Singh, R. Bajpai, and R. Bedi, "Alcohol sensing of tin oxide thin film prepared by sol-gel process," *Bulletin of Materials Science*, vol. 25, no. 3, pp. 231-234, 2002.
[35] I. El Zawawi, M. A. Mahdy, and E. El-Sayad, "Influence of film thickness and heat treatment on the physical properties of Mn doped Sb2Se3 nanocrystalline thin films," *Journal of Nanomaterials*, vol. 2017, 2017.
[36] B. K. B. Saifaddin, "Development of deep ultraviolet (UV-C) thin-film light-emitting diodes grown on SiC," UC Santa Barbara, 2018.
[37] J. A. Thornton, "High rate sputtering techniques," *Thin solid films*, vol. 80, no. 1-3, pp. 1-11, 1981.
[38] R. Hippler, H. Kersten, M. Schmidt, and K. H. Schoenbach, "Low temperature plasmas," *Eds R Hippler et al, Berlin: Wiley*, vol. 787, 2008.
[39] Y. Liu *et al.*, "Effects of annealing temperature, thickness and substrates on optical properties of m-plane ZnO films studied by photoluminescence and temperature dependent ellipsometry," *Journal of Alloys and Compounds*, vol. 848, pp. 156631, 2020.
[40] N. F. Habubi, Z. M. Abood, and A. N. Algamel, "Molar concentration Effects on the Optical and Structural Properties of nanostructural SnO2 Thin Films," *International Letters of Chemistry, Physics and Astronomy*, vol. 65, pp. 81, 2016.
[41] S. M. AL-Jawad, A. K. Elttayf, and A. S. Sabr, "The effect of annealing temperature on structural & optical properties of nanocrystalline SnO2 thin films prepared by sol-gel technique," *Engineering and Technology Journal*, vol. 34, no. 4 Part (B) Scientific, 2016.
[42] S. M. Al-Jawad, "Annealing Effect on Structure and Optical Properties of ZnO Thin Films Prepared by Spray Pyrolysis," *Eng &Tech. Journal*, vol. 33, 2015.

p-ISSN 1675-7939; e-ISSN 2289-4934